JOURNAL OF TISSUE ENGINEERING AND REGENERATIVE MEDICINE
J Tissue Eng Regen Med 2008; **2**: 430–435.
Published online 26 August 2008 in Wiley InterScience (www.interscience.wiley.com) **DOI:** 10.1002/term.115

RESEARCH ARTICLE

Role of NADPH oxidase in tissue growth in a tissue engineering chamber in rats

Hiroki Hachisuka[#], Gregory J. Dusting, Keren M. Abberton, Wayne A. Morrison and Fan Jiang*
Bernard O'Brien Institute of Microsurgery, University of Melbourne, Victoria, Australia

Abstract

Previously we described a subcutaneous arteriovenous loop (AVL)-based tissue engineering chamber system, which contains an intrinsic circulation circuit created by joining the proximal ends of the femoral artery and vein with a venous graft. We showed that nicotinamide adenine dinucleotide phosphate (NADPH) oxidase was involved in mediating neovascularization inside the chamber. However, the role of NADPH oxidase in tissue formation in the chamber is unknown. In this study, we examined the effects of gp91ds-tat, a peptidyl inhibitor of NADPH oxidase, on the growth of engineered tissue blocks, using a rat chamber model. Chambers containing the AVL were filled with Matrigel mixed with gp91ds-tat (*100 μM*) or the scrambled control peptide. At 14 days, in control chambers, most of the Matrigel was replaced by granulation tissues; gp91ds-tat treatment significantly reduced the level of reactive oxygen species and retarded the tissue formation process. Although the total number of blood vessels per unit cellularized area was not different between two groups, most vessels in gp91ds-tat-treated tissues had smaller lumens as compared to control. The total area occupied by vessel lumens was much less in gp91ds-tat-treated tissues (*10.3 ± 1.3*% in control vs. *1.7 ± 0.5*% in gp91ds-tat group; *$p < 0.001$*). *In vitro*, gp91ds-tat treatment reduced proliferation and migration of cultured microvascular endothelial cells. Our data suggest that inhibition of NADPH oxidase function retards tissue formation in the tissue engineering chamber, which may be related to the malformed new blood vessels in the engineered tissue. Copyright © 2008 John Wiley & Sons, Ltd.

Received 11 April 2008; Revised 18 June 2008; Accepted 19 June 2008

Keywords **NADPH oxidase; tissue engineering; arteriovenous loop chamber; angiogenesis; gp91ds-tat; rat**

1. Introduction

Our laboratory has developed a unique *in vivo* tissue engineering chamber system in rats, which has a genuine blood supply from the systemic circulation achieved by an artificial arteriovenous loop (AVL) (Cassell *et al*., 2001). The AVL is microsurgically constructed by cutting off the femoral artery and vein in the groin area and joining the two proximal ends with a venous graft obtained from the femoral vein of the contralateral side (see Figure 1). The chamber is secured under the skin and can be maintained within the body for up to 12 weeks (Cassell *et al*., 2001). Using this system, we have transplanted cells obtained from different sources and created a variety of vascularized soft tissues, including granulation tissues, fat, skeletal muscle and myocardium (Cassell *et al*., 2001; Messina *et al*., 2005; Dolderer *et al*., 2007; Morritt *et al*., 2007). A distinct feature of this chamber system is the vigorous angiogenic process that originates from the AVL (Jiang *et al*., 2007; Lokmic *et al*., 2007), which may be stimulated by the rapid fibrin exudation and inflammatory cell infiltration after AVL construction (Lokmic *et al*., 2007). This spontaneous angiogenesis into the newly formed tissue is vital for further expansion of the engineered tissue block inside the chamber.

*Correspondence to: Fan Jiang, Bernard O'Brien Institute of Microsurgery, 42 Fitzroy Street, Fitzroy, Victoria 3065, Australia. E-mail: fjiang@unimelb.edu.au
[#] Current address: Department of Orthopedic Surgery, Division of Clinical Medical Science, Graduate School of Biomedical Science, Hiroshima University, Hiroshima, Japan.

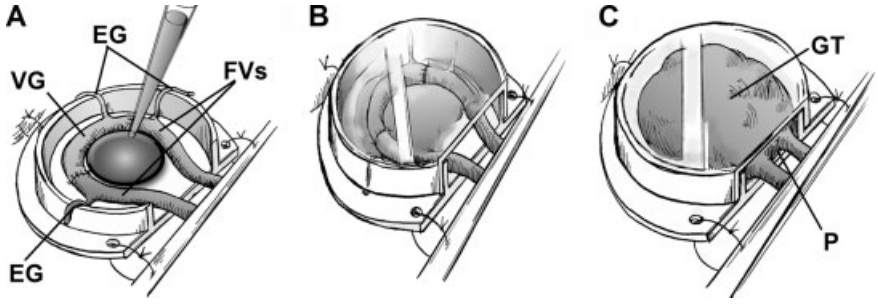

Figure 1. A diagram showing the configuration of the tissue engineering chamber containing an artificial arteriovenous loop (AVL). (A) An AVL has been placed in position in the chamber and Matrigel is being injected with a pipette tip. The AVL is microsurgically constructed by joining the two proximal ends of femoral artery and vein (FVs) in the groin area with a venous graft (VG) obtained from the femoral vein of the contralateral side. EG, epigastric branches. (B) A chamber filled with Matrigel and covered with the lid. (C) The granulation tissue block (GT) formed in the chamber and the femoral vessel pedicle (P)

Several lines of evidence have suggested that nicotinamide adenine dinucleotide phosphate (NADPH) oxidase may have a critical role in modulating angiogenic responses both *in vitro* and *in vivo* (Ushio-Fukai *et al*., 2002; Ago *et al*., 2004; Datla *et al*., 2007). NADPH oxidase, which is composed of the cytosolic p47phox and p67phox subunits, the membrane-bound Nox and p22phox, and a small G protein Rac, is a major intracellular source of reactive oxygen species (ROS) (Griendling *et al*., 2000). NADPH oxidase-derived ROS may act as signalling molecules modulating many aspects of cellular functions, such as proliferation, migration, differentiation and gene expression, while dysregulated NADPH oxidase function has been shown to be involved in the development of cardiovascular diseases, such as endothelial dysfunction, atherosclerosis and hypertension (Bedard and Krause, 2007).

In our previous study, we showed that the granulation tissue formation and neovascularization in the rat chamber model was accompanied by an increase in the expression of the Nox4 subunit of NADPH oxidase (Jiang *et al*., 2007). We also identified a strong expression of the Nox2 isoform in the endothelial cells of the new vessels (Jiang *et al*., 2007). Moreover, the NADPH oxidase inhibitor apocynin significantly inhibited the angiogenic response in the chamber (Jiang *et al*., 2007). Although adequate neovascularization of the chamber is critical for maintaining the viability of the engineered tissue, our previous study did not examine how NADPH oxidase affects the growth of the tissue in our chamber model. In the present study, we hypothesized that NADPH oxidase may be involved in modulating the growth of the engineered tissue. We employed a more specific peptidyl NADPH oxidase inhibitor, gp91ds-tat (Rey *et al*., 2001), to investigate the role of NADPH oxidase.

2. Materials and methods

2.1. Animals and chamber implantation

All procedures were carried out in compliance with the guidelines of the National Health and Medical Research Council (NHMRC) and approved by the institutional Animal Ethics Committee. Normal male Sprague–Dawley rats, each weighing 300–400 g, were randomly divided into control and gp91ds-tat-treated groups. Chamber implantation was performed as described previously (Jiang *et al*., 2007). Briefly, under general anaesthesia with ketamine and xylazine (75 and 10 mg/kg, respectively, i.p.), a transverse incision was made in the right groin to expose the femoral artery and vein from the level of inguinal ligament to the superficial epigastric artery. Both vessels were clamped proximally and cut off below the epigastric branch. A 15 mm long segment of femoral vein obtained from the left side was interposed between the divided recipient right femoral artery and vein, creating an arteriovenous shunt (AVL). The AVL was placed inside a polycarbonate chamber of about 0.55 ml in volume (see Figure 1).

2.2. Treatment with gp91ds-tat

A 10 mM stock solution of gp91ds-tat or a scrambled control peptide (all purchased from Auspep, Victoria, Australia) was prepared in dimethylsulphoxide (DMSO). After AVL construction, the stock solutions were thoroughly mixed with growth factor-reduced Matrigel (BD Bioscience, San Jose, CA, USA) to a final concentration of 100 μM, and the gel was applied into the chamber with a 1 ml pipette. Then the lid of the chamber was closed and chamber secured to the surrounding muscle.

2.3. Tissue processing

On day 14 after chamber implantation (Jiang *et al*., 2007), the chamber was exposed under general anaesthesia, the pedicle of femoral vessels tied up outside the chamber, and the tissues formed in the chamber were collected for analysis. After brief rinsing in cold saline, the weight and volume of the tissue were measured. Then the disc-like tissue was cut into halves in the middle between the top and the pedicle, and one was fixed in 4% paraformaldehyde for routine paraffin sectioning, while

DOI: 10.1002/term

the other half was embedded in OCT compound (Tissue-Tek, Torrance, CA, USA) for cryosectioning. In some of our experiments, we performed perfused fixation before tissue harvesting. However, we did not notice any difference of the tissue structure or morphology between perfused and non-perfused samples in the two groups. Therefore, perfused fixation was not consistently used for all of the samples.

2.4. Histology and morphometric analysis

Serial transverse sections of 5 μm in thickness were cut from the straight side of the tissue and stained with haematoxylin and eosin (H&E). To visualize blood vessels, the sections were stained with biotinylated *Griffonia simplicifolia* lectin (Vector Laboratories, Burlingame, CA, USA) as described (Jiang *et al.*, 2007). Briefly, the tissues were incubated with 3% H_2O_2 for 20 min to quench the endogenous peroxidase activity, followed by antigen retrieval with proteinase K (Dako, Glostrup, Denmark) for 4 min at room temperature. The biotinylated lectin (diluted 1 : 300) was applied for 30 min at room temperature. Then the slides were developed with horseradish peroxidase-conjugated streptavidin (Dako) and 3′-3-diaminobenzidine chromagen (Dako) and counterstained with haematoxylin. The total number of blood vessels in the whole section and the percentage area occupied by vessel lumens were counted using the Computer Assisted Stereological Toolbox (CAST) system (Olympus). The total dimension of the each section was also measured. Three slides were selected at random for one tissue and all parameters averaged.

2.5. Detection of superoxide

Superoxide anions were detected in 10 μm thick cryosections, as described previously (Jiang *et al.*, 2007), using dihydroethidium (DHE; Invitrogen, Carlsbad, CA, USA). After incubation with 10 μM DHE at 37 °C for 30 min, the slides were washed in saline and visualized using a fluorescent microscope (Axioskop2, Zeiss) with a 590 nm filter. All fluorescent images were taken with a digital camera (AxioCam MRc5, Zeiss) with fixed exposure settings. The specificity of the DHE fluorescence was confirmed by pretreating the sections with the superoxide dismutase mimetic Mn(III)TMPyP (100 μg/ml, from Cayman Chemical, Ann Arbor, MI, USA).

2.6. Cell migration and proliferation

Human microvascular endothelial cells (HMECs) were cultured in an endothelial cell culture medium (EGM-2 BulletKit, Cambrex Corporation) containing 5% fetal calf serum, as described previously (Jiang *et al.*, 2007). Cell proliferation was assessed with the CellTiter-96 AQueous One Solution kit (Promega) and measured as absorbance at 490 nm. Cell migration was assessed with a wound-healing assay with some modifications (Jiang *et al.*, 2007). Briefly, cells were cultured in six-well plates to confluent monolayer and serum-starved for 24 h. A wound was made by scratching a line across the monolayer with a pipette tip. The border of the wound was outlined manually at the bottom of the culture plate. After 24 h, the cells were fixed with cold methanol and stained with a Quick Dip staining kit (Fronine, NSW, Australia). The number of cells migrated beyond the border was counted in five or six randomly selected ×100 fields per well, using an inverted microscope (Olympus Model IX81F-2).

2.7. Statistical analysis

Data were expressed as mean ± SEM and analysed by unpaired *t*-test. A value of $p < 0.05$ was considered statistically significant.

3. Results

3.1. Gp91ds-tat inhibited tissue formation in the chamber

The total volume and weight of the fresh tissue just retrieved from the chamber did not differ between the control and treated groups (Figure 2). In the control chamber, most of the Matrigel was replaced by granulation tissue that filled the chamber space. A more careful analysis of the composition of tissue from gp91ds-tat-treated chambers revealed that a noticeable proportion of Matrigel remaining unorganized, indicating that the similar tissue weight and volume were likely to be an artifact caused by the residual Matrigel. However, it was impossible to clearly separate the gel from the tissues. To clarify this, we measured the mean cross-sectional area of the organized portion in H&E-stained slides. As shown in Figure 2C, the cellularized area of the sections of gp91ds-tat-treated tissues was much smaller that that of control tissues. The mean tissue cross-sectional area was reduced by 40% with gp91ds-tat treatment (Figure 2D). These data demonstrated that inhibition of NADPH oxidase function retarded tissue formation in the chamber.

To confirm that the concentration of gp91ds-tat used in the chamber can effectively inhibit NADPH oxidase activity, we measured the *in situ* superoxide level using DHE fluorescence. As shown in Figure 3, the superoxide level was markedly reduced in gp91ds-tat-treated tissues (the mean arbitrary fluorescence intensity being 28.8 ± 5.1 in control and 16.0 ± 1.5 in gp91ds-tat groups, respectively; $p < 0.05$, unpaired *t*-test; $n = 5$ animals in each group), suggesting that NADPH oxidase was the major source of ROS in the developing granulation tissue. Moreover, although DHE fluorescence was present over the whole cellularized area, we found that some ring-like structures expressed stronger DHE signals, which resembled the new blood vessels (Figure 3A).

DOI: 10.1002/term

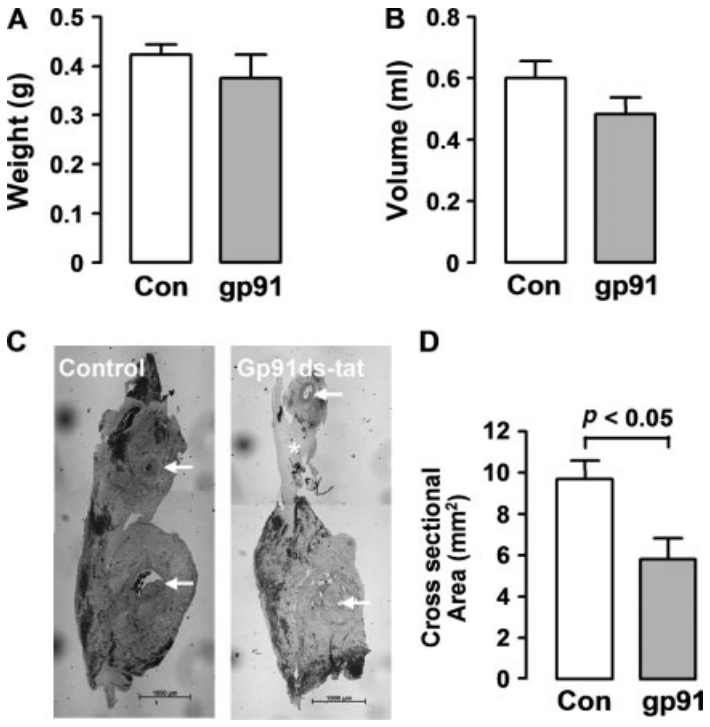

Figure 2. Effects of gp91ds-tat (grey bars) as compared to the scrambled control peptide (open bars) on tissue growth in the chamber. The wet weight (A) and total volume (B) of the fresh tissues were measured immediately after retrieval from the chamber. (C) H&E-stained transverse sections of the granulation tissues from control and gp91ds-tat-treated chambers, showing the different size of the cellularized area between the two groups. The lumen of the AVL is indicated by arrows. In the gp91ds-tat-treated tissue, some residual Matrigel can also be seen (*). Scale bar = 1 mm. The quantitative data of the cellularized cross-sectional area are shown in (D). $n = 5–6$ in each group

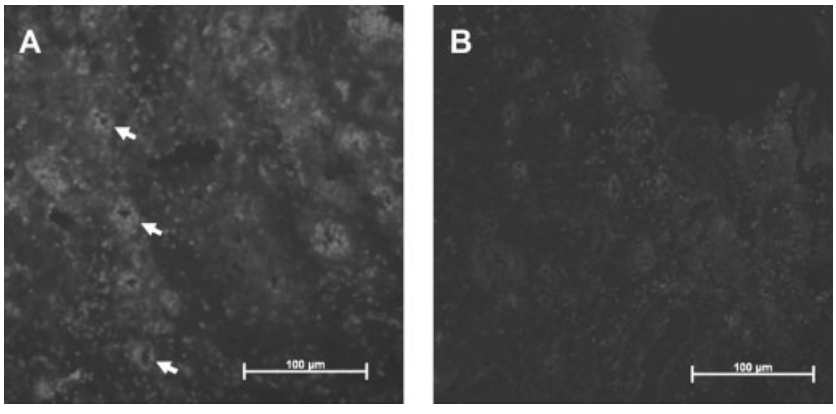

Figure 3. Dihydroethidium fluorescence images of cryosections from control (A) and gp91ds-tat-treated (B) tissues, showing the different levels of superoxide. Some ring-like structures expressing stronger DHE signals can be seen (arrows), which resemble the new blood vessels. Scale bar = 100 μm

3.2. Gp91ds-tat impaired neovascularization

Although the total number of blood vessels in the whole cellularized area was significantly less in gp91ds-tat-treated tissues as compared to controls, the vessel number per unit area was not different between the two groups (Figure 4). Interestingly, we found that the vessels in gp91ds-tat-treated tissues had much smaller lumen size as compared to controls (Figure 5). The total area occupied by vessel lumens was $10.3 \pm 1.3\%$ in the control group, in contrast to $1.7 \pm 0.5\%$ in the gp91ds-tat-treated group ($p < 0.001$, $n = 5–6$). In addition, we observed that in H&E-stained sections, a number of vessels in the control tissue seemed to have a thicker, multilayered wall (Figure 5A), indicating a process of vessel maturation. In contrast, these types of vessels were hardly visible in gp91ds-tat-treated tissues.

3.3. Gp91ds-tat inhibited endothelial cell proliferation and migration *in vitro*

In cultured HMEC cells, treatment with gp91ds-tat (100 μM) significantly inhibited cell proliferation, as

DOI: 10.1002/term

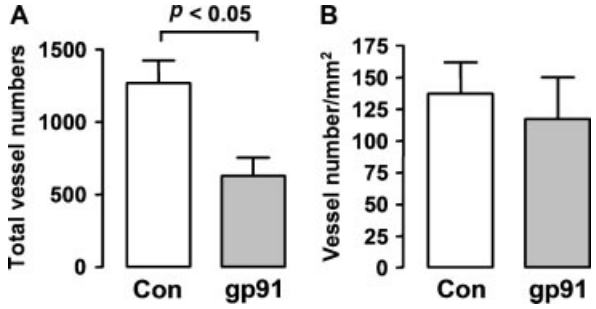

Figure 4. Effects of gp91ds-tat (grey bars) as compared to control peptide (open bars) on the total number of new vessels in the cellularized area (A) and the vessel density (number per unit area) (B) in the granulation tissue. $n = 5–6$

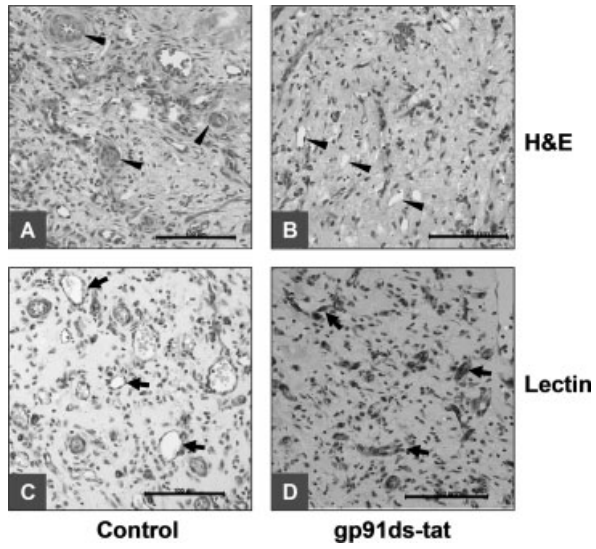

Figure 5. H&E and lectin staining of control and gp91ds-tat-treated tissues. In the H&E-stained sections, a number of vessels in control tissues exhibited a thicker, multilayered vessel wall (arrow heads) as compared to the vessels in gp91ds-tat treated tissues. This type of vessel was rare in gp91ds-tat-treated tissues. The lectin staining shows the profile of new blood vessels (arrows). Compare the different sizes of vessel lumen in control and treated tissues. Scale bar = 100 μm

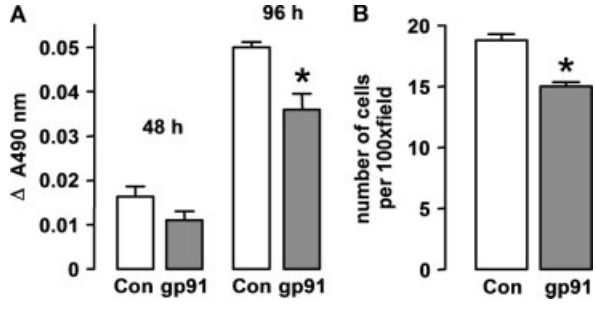

Figure 6. Effects of gp91ds-tat (100 μM) (grey bars) as compared to control peptide (open bars) on (A) cell proliferation and (B) cell migration in cultured human microvascular endothelial cells. Cell proliferation was expressed as the difference of absorbance at 490 nm between time 0 and 48 or 96 h later. Cell migration was assessed with a wound-healing assay and expressed as the average number of cells migrated beyond the border of wound per ×100 field. *$p < 0.05$ vs. control ($n = 3$)

shown in Figure 6A. Moreover, we found that inhibition of NADPH oxidase with gp91ds-tat also suppressed spontaneous cell migration in HMECs (Figure 6B).

4. Discussion

In this study, we examined the role of NADPH oxidase function in modulating tissue growth in our AVL chamber model. We found that inhibition of NADPH oxidase with gp91ds-tat significantly retarded tissue formation in the chamber. Survival and growth of the transplanted cells and tissues in the chamber require a functional vasculature capable of delivering sufficient oxygen and nutrients. Thus, limited angiogenesis may impede the growth of the engineered tissue graft. Our previous study showed that new blood vessels originating from the AVL could be identified as early as 3 days after chamber implantation, and the vessel density increased to a plateau from 7 days to 14 days. Consistent with our previous findings (Jiang *et al.*, 2007), here we demonstrated that gp91ds-tat treatment compromised the new blood vessel formation in the chamber. In particular, we found that the vessels in gp91ds-tat-treated tissues had much smaller lumen size as compared to controls, although the number of blood vessels per unit area was not different between the two groups. Our data suggest that the malformed new blood vessels may contribute to the delayed tissue formation in gp91ds-tat-treated chambers. It should be noted, however, that we did not directly measure the functions of these new blood vessels (e.g. the blood flow in the chamber); thus, a causal role of vessel malformation in the reduced tissue growth could not be established. Moreover, our data could not exclude that NADPH oxidase might also modulate proliferation of stromal cells, as suggested by others (Adachi *et al.*, 2005; Manabe *et al.*, 2007).

Previously we found that the tissue formation in the chamber was accompanied by a concomitant increase in expression of the Nox4 subunit of NADPH oxidase (Jiang *et al.*, 2007), which is important in mediating ROS generation in both vascular endothelial and smooth muscle cells (Ago *et al.*, 2004; Ellmark *et al.*, 2005; Jiang *et al.*, 2006). On the other hand, we have also identified a localized expression of Nox2 in the endothelial cells of the newly formed vessels and in a subpopulation of infiltrating monocytes (Jiang *et al.*, 2007). All these cellular components may contribute to the total ROS production in the granulation tissue. In consistency with our previous study (Jiang *et al.*, 2007), we also found that some ring-like structures exhibited higher levels of superoxide generation (stronger DHE signals), indicating an enhanced NADPH oxidase activity in the newly formed blood vessels. The effectiveness of gp91ds-tat in inhibiting NADPH oxidase activity in the chamber was confirmed by the finding that the *in situ* superoxide level was markedly reduced in gp91ds-tat-treated tissues.

DOI: 10.1002/term

Several lines of evidence suggest that NADPH oxidase-dependent redox signalling has an important role in modulating angiogenesis. For example, Tojo *et al*. showed that the angiogenic response stimulated by tissue ischaemia was significantly impaired in Nox2-deficient mice. Recently, we demonstrated that inhibition of Nox4 expression reduced the *in vitro* angiogenic responses in cultured human endothelial cells (Datla *et al*., 2007). Moreover, we have found that the proangiogenic effects of Nox4 are at least partly mediated by enhanced receptor tyrosine kinase phosphorylation and the activation of extracellular signal-regulated kinases. In line with these findings, our *in vitro* experiments in cultured microvascular endothelial cells demonstrated that gp91ds-tat treatment significantly inhibited both cell proliferation and migration (Figure 6), suggesting that impaired angiogenic properties of endothelial cells might underlie the vessel malformation in gp91ds-tat-treated chambers. Moreover, we observed that in control tissues, a number of vessels appeared to have a multilayered vessel wall (Figure 5A), which was rare in gp91ds-tat-treated tissues, indicating that NADPH oxidase-dependent mechanisms might also be involved in vessel maturation.

Altered inflammatory responses in the chamber may be another possible mechanism by which gp91ds-tat modulates angiogenesis. In chambers without Matrigel addition, fibrin exudation and inflammatory cell infiltration occurred rapidly after the AVL construction (Jiang *et al*., 2007; Lokmic *et al*., 2007). Obvious leukocyte accumulation was also observed in the Matrigel in gel-filled chambers preceding the granulation tissue formation (Jiang *et al*., 2007). This inflammatory response is thought to be a major intrinsic stimulus for the angiogenic process in the chamber. However, in our previous study we found that apocynin, another NADPH oxidase inhibitor, which similarly inhibited neovascularization of the chamber as gp91ds-tat, had little effect on inflammatory cell accumulation in the Matrigel (Jiang *et al*., 2007). Moreover, the inhibitory effect of gp91ds-tat on NADPH oxidase activation is much weaker in leukocytes than that in vascular cells (Rey *et al*., 2001), although the reason for this difference is unclear. All these findings suggest that a reduced inflammatory response is unlikely to have a major contribution to the inhibitory effects of gp91ds-tat on angiogenesis and tissue formation in the chamber.

In summary, we found that inhibition of NADPH oxidase with gp91ds-tat significantly reduced the tissue development in our AVL chamber model, and this might be partly because of the malformation of new blood vessels (smaller vessel lumens). A limitation of the present study was that we did not distinguish the individual roles of different NADPH oxidase isoforms (e.g. Nox2 vs. Nox4), because gp91ds-tat is a non-specific NADPH oxidase inhibitor. Nonetheless, our data indicate that a normal NADPH oxidase function is required for optimal tissue formation in the tissue engineering chamber.

Acknowledgements

The authors thank Jason Palmer and Srinivasa Raju Datla for technical assistance in tissue processing and DHE fluorescence imaging, respectively. This work was funded by project grants from the National Health and Medical Research Council (NHMRC) of Australia, and grants-in-aid from the National Heart Foundation of Australia. G.J.D. also receives a Principal Research Fellowship from NHMRC. The authors declare no conflict of interest.

References

Adachi T, Togashi H, Suzuki A, *et al*. 2005; NAD(P)H oxidase plays a crucial role in PDGF-induced proliferation of hepatic stellate cells. *Hepatology* **41**: 1272–1281.

Ago T, Kitazono T, Ooboshi H, *et al*. 2004; Nox4 as the major catalytic component of an endothelial NAD(P)H oxidase. *Circulation* **109**: 227–233.

Bedard K, Krause KH. 2007; The NOX family of ROS-generating NADPH oxidases: physiology and pathophysiology. *Physiol Rev* **87**: 245–313.

Cassell OC, Morrison WA, Messina A, *et al*. 2001; The influence of extracellular matrix on the generation of vascularized, engineered, transplantable tissue. *Ann N Y Acad Sci* **944**: 429–442.

Datla SR, Peshavariya H, Dusting GJ, *et al*. 2007; Important role of Nox4 type NADPH oxidase in angiogenic responses in human microvascular endothelial cells *in vitro*. *Arterioscler Thromb Vasc Biol* **27**: 2319–2324.

Dolderer JH, Abberton KM, Thompson EW, *et al*. 2007; Spontaneous large volume adipose tissue generation from a vascularized pedicled fat flap inside a chamber space. *Tissue Eng* **13**: 673–681.

Ellmark SH, Dusting GJ, Fui MN, *et al*. 2005; The contribution of Nox4 to NADPH oxidase activity in mouse vascular smooth muscle. *Cardiovasc Res* **65**: 495–504.

Griendling KK, Sorescu D, Ushio-Fukai M. 2000; NAD(P)H oxidase: role in cardiovascular biology and disease. *Circ Res.* **86**: 494–501.

Jiang F, Roberts SJ, Raju Datla S, *et al*. 2006; Nitric oxide modulates NADPH oxidase function via heme oxygenase-1 in human endothelial cells. *Hypertension* **48**: 950–957.

Jiang F, Zhang G, Hashimoto I, *et al*. 2007; Neovascularization in an arteriovenous loop-containing tissue engineering chamber: role of NADPH oxidase. *J Cell Mol Med* (14 December 2007; Epub ahead of print).

Lokmic Z, Stillaert F, Morrison WA, *et al*. 2007; An arteriovenous loop in a protected space generates a permanent, highly vascular, tissue-engineered construct. *FASEB J* **21**: 511–522.

Manabe S, Okura T, Fukuoka T, *et al*. 2007; Antioxidative effects of azelnidipine on mesangial cell proliferation induced by highly concentrated insulin. *Eur J Pharmacol* **567**: 252–257.

Messina A, Bortolotto SK, Cassell OC, *et al*. 2005; Generation of a vascularized organoid using skeletal muscle as the inductive source. *FASEB J* **19**: 1570–1572.

Morritt AN, Bortolotto SK, Dilley RJ, *et al*. 2007; Cardiac tissue engineering in an *in vivo* vascularized chamber. *Circulation* **115**: 353–360.

Rey FE, Cifuentes ME, Kiarash A, *et al*. 2001; Novel competitive inhibitor of NAD(P)H oxidase assembly attenuates vascular O_2^- and systolic blood pressure in mice. *Circ Res* **89**: 408–414.

Ushio-Fukai M, Tang Y, Fukai T, *et al*. 2002; Novel role of gp91(phox)-containing NAD(P)H oxidase in vascular endothelial growth factor-induced signalling and angiogenesis. *Circ Res* **91**: 1160–1167.